Operating Characteristics of a Passive, Bidirectional Overrunning Clutch for Rotary Joints of Robots

Torsten Siedel*, Dusko Lukac†, Tim Geppert‡, Christian Benckendorff§, and Manfred Hild¶
* ‡ § Neurorobotics Research Laboratory
Humboldt-Universität zu Berlin, Unter den Linden 6, 10099 Berlin, Germany
Email: siedel|geppert|benckend@informatik.hu-berlin.de
† Rheinische Fachhochschule Köln gGmbH
Department of Robotics and Mechatronics, Vogelsangerstr. 295, 50825 Cologne, Germany
Email: lukac@rfh-koeln.de
¶ SONY Computer Science Lab, 6, Rue Amyot, 75005 Paris, France
Email: hild@csl.sony.fr

***Abstract*—For the development of robots the mode of assembly and the effectiveness of their joints are of elementary significance. To enable powerful movements, strong torques are required which, when employing electromechanical actuators, are generated by high-capacity motors in combination with adequate speed transformations. Furthermore, such drive systems have to withstand even very high external loads which can be caused by uncontrolled motions, e.g., by stumbling of a humanoid robot. In particular the gears have therefore to be of robust construction. Likewise, the energy efficiency of the drive systems plays a decisive role for the perseverance of robots. The latter underlies a negative impact especially by frictional losses of highly transforming gears. In the present publication a novel design of a clutch is described. It has been developed with the goal to equally meet the requirements both of high energy efficiency and capacitance of robots. Apart from its configuration, this paper mainly deals with the technical performance of the new clutch, especially in combination with the actuator used.**

***Index Terms*—verrunning clutch, energy-efficient actuation, shock absorbing, passive decouplingverrunning clutch, energy-efficient actuation, shock absorbing, passive decouplingo**

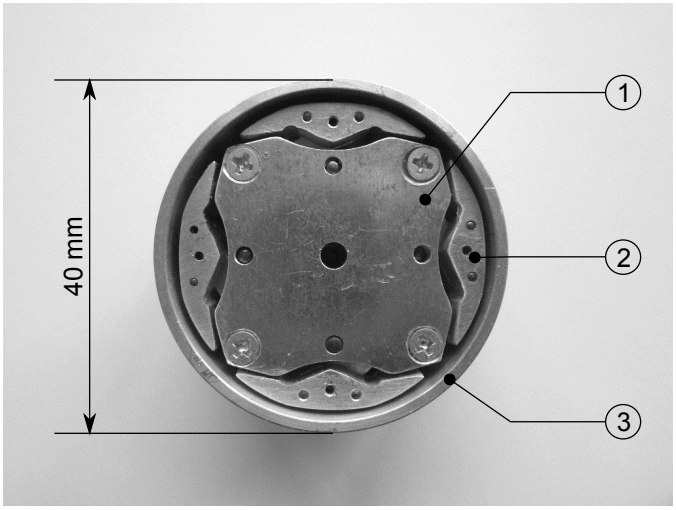

Fig. 1. The overrunning clutch with opened housing. Marked: The torque transmitting components, drive shaft (1), four wedges (2), and output hub (3). To illustrate the dimensions of the clutch, the output hub diameter is signed.

I. Introduction

The configuration of joints and the design of the drive system play a crucial role for the performance of robots. Essential requirements are both the producibility of strong torques and a high mechanical tolerance against shocks caused by external forces. This in particular applies to long limbs of large humanoid robots. Likewise, a high energy efficiency of the drive system is needed to attain an appropriate perseverance of the robot. Such requirements can be in conflict with each other when using electro-mechanical drive systems based on motor-gear assemblies. Strong torques are usually generated by gears with a high transformation of motor speed. This, however, can significantly reduce the drive system's energy efficiency. Furthermore, since the actuator systems are often rigidly coupled to the joints, they have to be turned during all joint motions as well. This especially exerts a negative impact on the efficiency of pendulous motions such as during the leg's swinging phase. An exception in this context represents the "'BioRob"' arm of the Technical University of Darmstadt [4]. This arm can undock a slowly turning positioning drive system from the joint to enable rapid movements induced by the main drive system. Though not all drives are being uncoupled from the joint, this pivot design already leads to an improved performance when both dynamic and precise movements are required. To interrupt a torque transmission, numerous types of clutches can be used the prevalent principles of which are dealt with under [8].

Compared to these devices, the clutch described in this paper represents a distinct novelty. It has been developed especially for the use with robots. In the first part of this paper, the functional principle of this clutch is explained. Thereafter we describe the testing equipment and the actuator serving as drive system with which all investigations had been carried out. Finally, experimental data on the functional properties of the clutch are presented and discussed.

978-1-4577-0746-9/11/$26.00 ©2011 IEEE

II. Principle of Function

Clutches used for torque transmission in general can be divided into two categories. First, clutches based on an active functional principle. They need an additional control signal to couple or uncouple and comprise devices such as magnetic clutches (as, e.g., being used with the BioRob arm [4]), or constructions employing electro-rheological fluids [6], [9]. Second, passive clutches which do not require a special signal for the coupling process. The clutch described in this paper belongs to this second category, its operating mode being based on the principle of overrunning. This principle is well known from various models, the most famous of these is that of a bicycle. The purpose of such clutches is to transmit torque forces in a single direction only. For their constructive realization mainly four different variants are being employed. These are spring clutch, roller or ball clutch, sprag clutch, and ratchet clutch, respectively [10]. For application with robots, however, a bidirectionally working overrunning clutch is necessary. Such types of overrunning clutches are comparatively rare. Moreover, there is only little documentation about such clutch types, most of it can be found in the patent literature [7], [11]. Such clutches usually rely in torque transmission on the same principles as their unidirectionally operating counterparts.

With the clutch described here, a novel type of locking mechanism has been realized. Essentially it is based on a force-fit connection.

A. Constructive Details

The clutch model used for experimental purposes has an outer diameter of 40 mm, with 25 mm in length, and a weight of approx. 50 g. The individual building elements consist either of aluminum, or ABS plastics, respectively, the latter of which having been manufactured by the so-called "rapid prototyping procedure".

Fig. 2 shows the inner clutch assembly by four cutaway views. Panel (A) depicts a cutaway view through the middle of the clutch, where the lower part of the drive shaft (1), a wedge (2), and the output hub (3) can be seen. (a) Denotes the main clutch axle, and (b) the axle around which the wedge can turn. In panel (B), all four wedges can be seen, and in panel (C) the inner assembly via the second part of the drive shaft is depicted when closed. The wedges are located in the middle between both parts of the drive shaft which enables to better keep the wedges in their turning points (b). Panel (D) includes the synchronization cross element which aligns all wedges among each other, and also provides a friction contact with the gear housing. Furthermore, this friction contact prevents an accidental snapping of the wedges into their end positions. The construction and assembly of the frictional contact has been described in detail elsewhere [2] and is therefore not considered here further.

The mode of operation is visualized in Fig. 3 and described as follows: If the wedges are in their neutral positions, as shown in the center panel, the connection between drive input and output is released. The output hub can therefore freely move in both directions of rotation. If the drive shaft turns

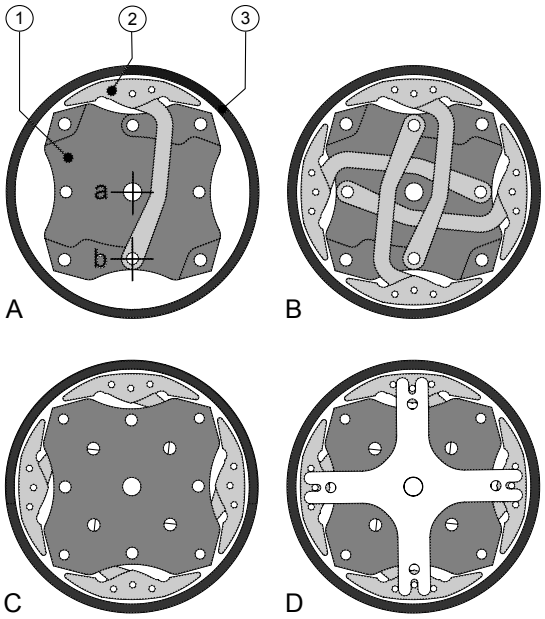

Fig. 2. This figure shows the inner assembly of the clutch. In panel (A) the three basic components responsible for the torque transmission are depicted. (1) denotes the drive shaft, (2) a wedge, and (3) the output hub, respectively. Both drive and output hub rotate around the axle (a). Wedge (2) can additionally slew round axle (b). The contact face of the drive shaft (2) has been teflonized for a facilitated slip-in of the wedge (2) into its final position. For a good power transmission, the inner surface of the driven hub has been rubberized. Panel (B) shows all four wedges, and panel (C) the same part but being covered by the second part of the drive shaft. Panel (D) shows the assembly in connection with the synchronization cross element which ensures the radially symmetrical alignment of the wedges. In addition, this element or part allows for a contact to the mechanical "grounding" to avoid an accidental clutching-in of the wedges.

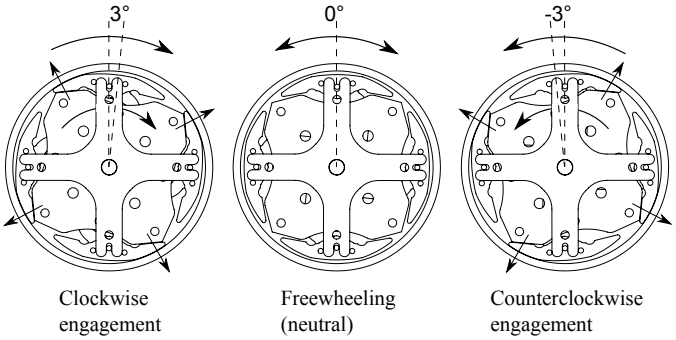

Fig. 3. Illustration of the three operating modes of the clutch. Left panel: The drive shaft rotates clockwise, whereby the wedges generate a transmission of torquer between drive and output hub. Center panel: The wedges are located in their neutral position, thus disconnecting drive and output hub, thus suspending torque transmission by overrun. Right panel: Situation analogous to that shown in the left panel except that the rotation of both drive shaft and output hub is invers.

clockwise for 3° (see Fig. 3 left panel), the wedges lock between the contact faces both of the drive shaft and the interior of the output hub. This leads to a transmission of power between the shaft and the hub, thus transferring torque. If the drive shaft starts to turn in the opposite direction, i.e., counterclockwise, in the first moment the wedges are first temporarily being released into their neutral position but

immediately thereafter locked in their opposite end position. Then, again power and torque can be transmitted from the drive and the output hub. In both end positions of the wedges, it may occur that the output hub rotates faster, e.g., due to external forces, than the drive shaft. Such a condition is tolerated by the clutch since the wedges are then being drawn out of their end positions and transmission of power is interrupted.

To ensure a smooth slide of the wedges into their end positions, the areas both of wedges and drive shaft at the contact faces are teflonized. At these contact faces, torque is being transmitted by form fit since the wedges, in this position, cannot further elbow. Between output hub and wedges, in contrast, torque is being transmitted by force fit. For this reason, the interior of the output hub is rubberized in the contact area.

III. Experimental Set-up

To determine both the functional characteristics of the clutch and of the actuator used we have developed a testing array the configuration of which is largely based on similar arrays described under [3], [5]. In fig. 4 the design of this testing array is illustrated schematically. Both ahead and behind the clutch (mark (3) of fig. 4) an optical angle sensor ((2) and (5)) is installed. For determining the output torque, the output hub of the clutch is connected with a torque sensor which measures the torque transferred to the output shaft (6) of the testing assembly. This torque sensor is angle-independent and works with loads of up to 5 Nm. For conducting reference tests it is possible to remove the clutch and to directly connect the actuator rigidly with the torque sensor. Furthermore, the testing array can alternatively be connected with either a pendulum, a wire rope, or a gyrating mass, respectively. Optionally, the output shaft can be fastened as well.

IV. Actuator

The actuator (cf. mark (1) of fig. 4) is based on a digital servomotor type RX-28 of Robotis Co., South Korea. It has integrated power electronics to activate its DC motor which, in combination with a spur gear, generates the mechanical output rating. The RX-28 further contains a temperature sensor for monitoring the drive properties. As already described under [1], the actuator is controlled by a PC via an electronic interface named AB3D. This interface also allows the measurement of the whole servomotor's current flow. With its firmware as pre-installed by Robotis the RX-28 unit can be simply accessed. The motor can be controlled electronically via the H bridge. It also provides a brake and release mechanism. In the brake mode the two electrical motor connections are short-circuited by the H bridge. This way the motor becomes an eddy-current retarder against an externally generated rotation. In the release mode, the connection between both electrical motor contacts is interrupted. This prevents the generation of an eddy current during motor rotation, and the RX-28 output drive can therefore be freely rotated. A new firmware created by ourselves in addition enables the regulation between the brake and release mode and thus allows for the desired strength adjustment of the eddy-current retarder.

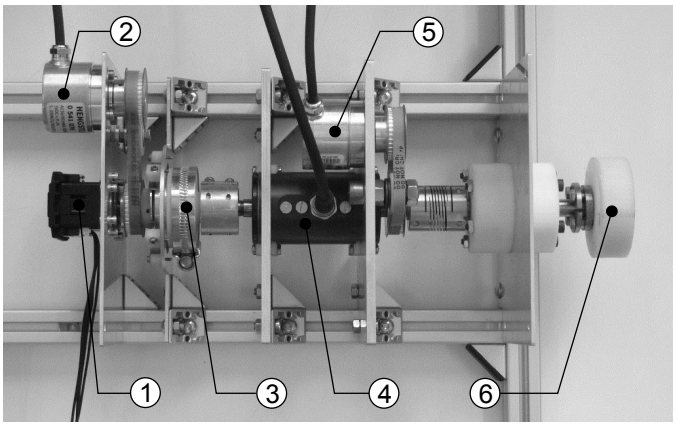

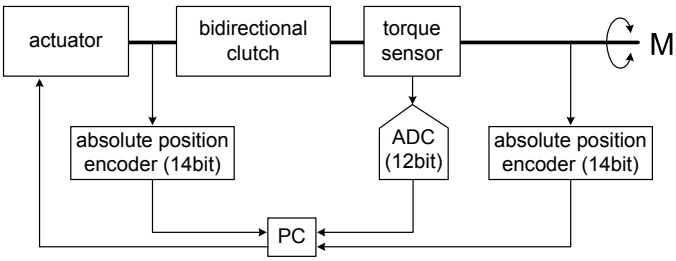

Fig. 4. Upper part, arrangement of the measuring section with markings of the essential components. (1) Servomotor RX-28, (2) angle sensor for determining the angle in front of the clutch, (3) clutch, (4) torque sensor, (5) angle sensor for determining the angle behind the clutch, (6) output (optionally to be combined with either a wire rope or a pendulum). Lower part: Schematic illustration showing the arrangement of all measuring section components. The angle sensors work with an accuracy of 14 bit, and the signal of the torque sensor is detected with an accuracy of 12 bit.

With a DC motor the driving speed depends on the motor voltage, and the torque on the motor current flow. For the subsequent determination of the coupling properties the torque generated by the servomotor is of particular interest. We have therefore mainly concentrated on the experimental assessment of the torque characteristics, especially aiming at a deduction of the output momentum provided by the servomotor and the AB3D interface from the sensor signals. In such an experiment the servomotor is rigidly connected with the shaft of the torque sensor. Also, the output shaft of the test array is completely fastened. The test sequence is illustrated in in fig. 5 and proceeds as follows. The servomotor is being accessed by pulsed ramp signals ranging from 0 to 100% of the motor voltage U.

A complete ramp sequence takes 12 seconds and is divided into 20 individual pulses, each of the pulses being elevated in U by 5% over the proceeding one. Pulsation occurs in $60ms$ intervals, where in between the individual pulse phases the voltage decreases for $10ms$ to 0%. The torque produced by the motor, as well as the motor's temperature and current flow

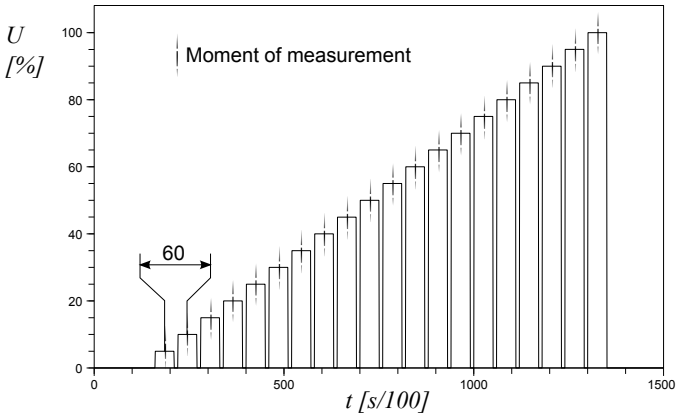

Fig. 5. Voltage signal ramp during a control of the RX-28 for the determination of its torque characteristics. The abscissa represents the time in $s/100$, and the ordinate the motor voltage U in %. A ramp consists of a total of 20 impulses with each impulse being applied in a time interval of 0.6 seconds. All measurements for data collection were performed after the half of an impulse duration.

are measured at 50% duration time of every pulse. All together ten such ramps are passed through in sequence in one test. One test therefore takes 130 seconds. As the servomotor gradually grows warmer during this time, the subsequent test is only conducted after the temperature of the servomotor has dropped to ca. $40°C$ again. In total the test is repeated ten times. Due to the quasi static test run measurement errors, caused by a stick-slip effect, or/and increased background noise of the torque sensor output signal can be avoided. At a continuous voltage vs. time ramp increase such undesirable factors could strongly falsify the metered values.

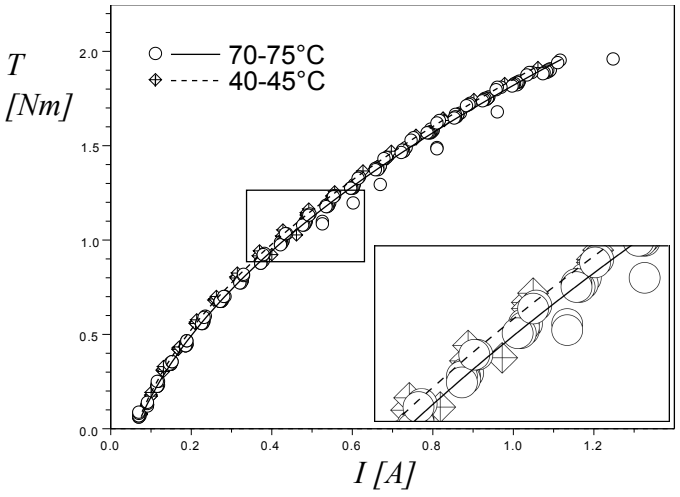

Fig. 6. Torque values T over current values I for two different temperature ranges. The discrete data pairs have been fitted by a polynomial function of 2nd order.

The data obtained from two temperature intervals are shown in the diagrams of fig. 6. The first temperature interval, 40 to $45°C$, is representative of the servomotor's operating temperature. As an upper limit of the operating temperature, an interval from 70 to $75°C$ was chosen. The absolute upper limit of the RX-28 operability is at $80°C$.

Further, the fitted curves are shown for both temperature intervals. They are based on a quadratic polynomial in the torque, which parameters are obtained by the method of least squares. The uncertainties of the parameters are approximated by uncertainties determined from methods of linear regression in first order. The latter are usually of the same order as those calculated from quadratic regression and therefore can easily be used to compare both curves in this case. The maximal uncertainty is determined to 0.040. The maximal difference in the parameters for the two most farthest temperature intervals is 0.023 and within the range of the uncertainty of a single parameter. Hence, even if we can guess a slight temperature dependence from the measured mean values in the current–torque relation, the uncertainties in the fit parameters are too huge to take this dependence into account. For a more detailed discussion of the temperature influence on the measurements one has to enlarge the interval of taken temperature data. Here we can take the mean of the fit parameters of the two discussed curves to get a mean current–torque relation and eliminate the temperature dependence:

a = 0.0013 (constant)
b = 0.0237 (linear)
c = 0.0054 (quadratic)

This relation is the base for the application of the RX-28 in connection with the coupling and shows that the measurement of the current at static states yealds values for the output torque and vice versa.

V. Evaluation of Clutch Characteristics

In the following we will discuss the slippage depending on the torque level. Subsequently, we will present an experiment for determining the decouple characteristics in correspondence with the characteristics of the RX-28.

A. Slippage

As mentioned before, the clutch described here transmits a torque by means of frictional connection. This principle allows for a continuously variable clutching-in whereby, in every angular positioning, the wedges ensure the torque transmission between input shaft and output hub. As a consequence of the use of pairs of different materials the traction-generating contact faces consist of (aluminum and elastomers) a sliding between both faces can occur depending on the strength of the torque being transferred. This represents the slippage of the clutch which expresses itself externally by an increasing angular difference or twist of the input and output shaft against each other.

To determine the slippage the output shaft of the testing apparatus is being kept in a fixed position. On the output wheel a rope is coiled up which, at its end, bears a weight. This generates a torque T which leads to a gradual kneeling of the weight element. The mass of the weight is then increased stepwise and the angular difference between the sensors (2) and (5) (cf. fig. 4) measured. Derivatization of the obtained

values yields the slippage given as angular velocity ω. The characteristics of the slippage behavior is shown in figure 7 7.

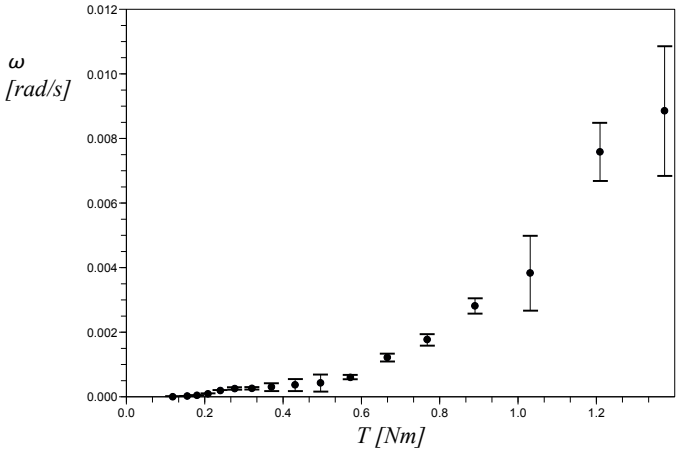

Fig. 7. The clutch's slippage depends on the transmitted torque T, which arises from the wire rope and the mass during the experimental setting. Slippage is given by the rotational velocity ω. Five experimental trial have been conducted per data point. The latter are given along with their standard derivation.

Slippage occurs when the torque exceeds ca. $0.2Nm$. From there on, slippage increases steadily. The diagram does also exhibit a non-linear relationship between torque and angular velocity, and a significant increase in standard deviation at high torque values. The maximum slippage found was about $0.012rad/s$ which is comparatively low against the maximum angular velocity of RX-28 ($0.5rad/s$ at $1.4Nm$ load). This test therefore shows that the angular velocity of slippage does not reach or exceed that of the RX-28 even at full load. It furthermore demonstrates that, despite of slippage, it can be ensured that the drive system can maintain a given position at a load of up to $1.4Nm$.

B. Engagement Characteristics

As mentioned before, the clutch presented here functions according to a passive coupling principle and therefore does not depend on an external electrical signal. To switch from a coupled to an uncoupled state it is only necessary to interrupt the power transmission between input shaft and output hub. This is brought about by moving the wedges into their middle or neutral position (cf. fig. 3). This reset motion can be effected by an active movement of the servomotor. However, the particular clutch assembly and the use of an elastomer for power connection provide an effect of elasticity which promotes an automatic uncoupling. If the clutch is burdened with a torque load, a spring tension builds up within the clutch. If the torque of the servomotor is spontaneously abolished, the clutch relaxes and turns back the input shaft by its resilience. The angle of resetting $\Delta\alpha$ depends both on the initial tension of the clutch and the braking power of the servomotor. In case the clutch has to transmit a higher torque, the angle $\Delta\varphi$, as shown in fig. 8, of the wedges around axle (b) of fig. (2) increases concomitantly since they are being pressed more strongly against rubberized interior wall of the output hub. Consequently, for a safe uncoupling the reset angle of the drive shaft is torque-dependent.

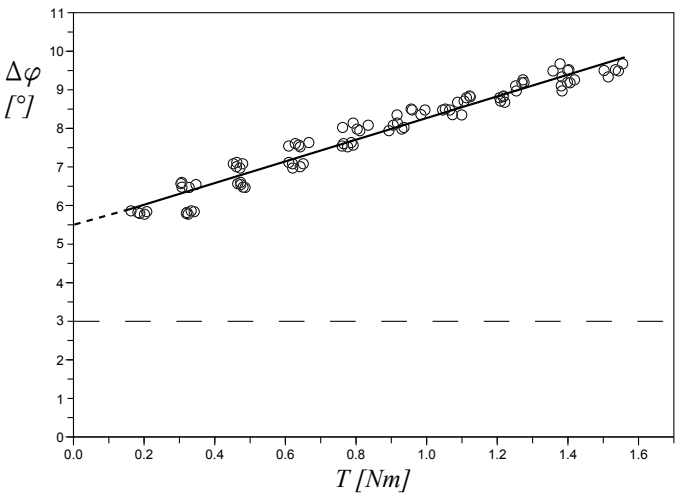

Fig. 8. Relation between angle of coupling-in and clutch torque. T, Torque of the clutch; $\Delta\varphi$, difference of angles between the neutral and extreme (end-point) clutch positions. The theoretical $3°$angle of coupling-in is marked by a dashed line.

The next experiment reveals the consequence of this effect. In this case, the output drive of the test array again had been fixed in one position. Then, the servomotor was accessed with increasing, alternating impulses. The duration of a single impulse was very short, i.e., $0.25s$, in order to minimize influences by a slippage of the clutch. At the half of the impulse duration both the torque and the drive angle were measured. The angle of coupling-in resulted from the half of the angle difference between a value pair of a positive and a negative peak with equal amplitude. For each coupling-in angle the torque was measured. These pairs of values are shown for both rotation directions in the diagram of fig. 8. As can be seen, the coupling-in angle increases by approx. $6°$up to a value of $10°$. Fig. 3 reveals, that theoretically a angular difference of $3°$is necessary to reach the final position. This is shown by a line in Figure 8. Actually, this theoretical value has been exceeded during the experimental testing, which can be explained by additional slippage between the wedges and the driving shaft. The data set has been approximated by a straight line, so that the slippage characteristics can more easily been used in the following examinations.

In the second experiment with the coupling, the back-set effect was determined by the elastic characteristic of the coupling in dependence of the torque and the release mode. For the realization of this experiment the servomotor was controlled by a pulsed ramp again, like in the performance test of RX-28, as presented in fig. 9. The uncoupling takes place after the end of every voltage pulse. During the uncoupling, the servomotor becomes during the unattended time switched between the pulses in the release mode (see fig. 9 below). During the traverse of a ramp the value of the release mode remains always the same. In the experiment ten ramps becomes traverse and the value of the release modes is increased

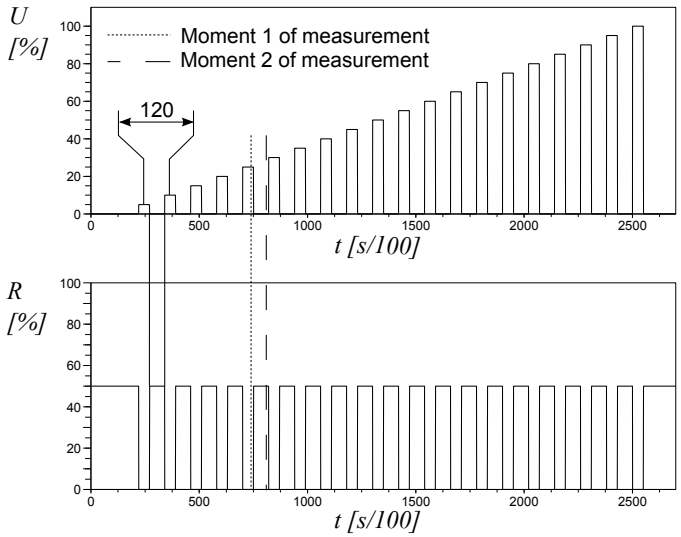

Fig. 9. Description of the driving signals which control the motor voltage (top) and the activation of the release mode (bottom). Time is given in units of $s/100$. The motor voltage U is given as a normalized percentage of the maximum value. The same is true for the control of the release mode R. The control pulses are spaced by $1.2\,\mathrm{s}$. Between the pulses, U is set to zero and R to 50%.

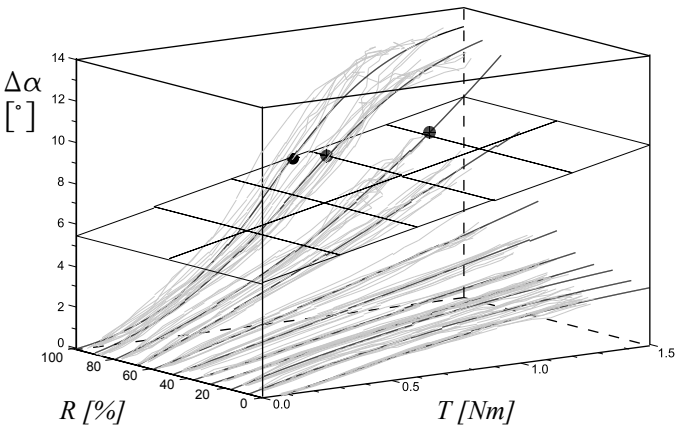

Fig. 10. Results of the uncoupling experiment within the testing array. The value R for the release mode was predefined and varied with equidistant steps of 10%. The torque T was applied by the servomotor which was also controlled by predefined values. After uncoupling of the clutch by switching to the corresponding value for the release mode, the maximum angle difference was measured. Every single run of the experiment is shown as grey curve; an approximated function for every array of curves having the same value for R is displayed in black. Additionally, a plane in which the uncoupling should be successful is indicated; according to fig. 8, the plane increases linearly in relation to the torque and is orthogonal to the plane which is spanned by $\Delta\alpha$ and T. The points where the approximated functions cross the linear plane are highlighted by black dots, to clarify for which torque a passive uncoupling is possible and which value R should be chosen for the release mode, respectively.

on traversing a ramp always by 10%. In order to capture the quality of the uncoupling, shortly before the end of a voltage pulse (fig. 9 moment 1) the torque and the angle of the drive shaft becomes grasped. Then it is waited briefly that the torque and therefore the internal tension of the coupling becomes diminished and shortly before the next pulse (fig. 9 moment 2), once more the angle of the drive shaft becomes measured. The difference of these both angle measurements as well as the grasped torque proves a measuring value. Traversing a ramp function generates a total of 20 measured data about the complete control area of the servomotor and of a value of the release mode. Every ramp traverses for a value of the release mode at least 10 times. The single curves derived from it are displayed in the graph 10 and are for every value of the release mode averaged. In addition, a linear rising layer, orthogonal to $\Delta\alpha - T$ layer, is stretched, which displays the angle $\Delta\varphi$ in dependence of the torque T.

Out of the intersections of the single curve and the layer it is evident with which torque T a suitable value R for the release mode must be adjusted in order to realize the uncoupling into the neutral position of the coupling. As is to be seen, cutting data do not originate for the whole torque range but only with an increased torque and as well as with the high value of the release mode. Out of it, it can be concluded that the generated spring tension is only adequate for a sufficient back set movement of the drive shaft, with a high release mode, in order that the coupling uncouples. For uncoupling in the low torque range, e.g., an active back set movement by the servomotor can allow uncoupling.

VI. Conclusion

In the present paper the construction, the functionality, the slippage as well as the uncoupling of a passive, bidirectional neutral coupling for the use in rotary joints of robots was explained. For the realization of the experiments with the coupling, a servomotor of the type RX-28 was used, whose torque characteristic was likewise determined experimentally. It has been determined, that in spite of passive construction style of the coupling, uncoupling is possible without active control of the impulse in the upper torque range. In order to realize this, two requirements must be given. First, before uncoupling, the enclosed torque value must be shortly determined. Secondly, the brake effect of the impulse must be adjustable. The torque test with RX-28 has shown, that for the determination of the torque, the measurement of the approximately current consumption of the servomotor, in the connection with the before ascertained square interrelation between current and torque, can be used. The brake effect can be adjusted by the regulation between brake and release mode. To attain this possibility a new firmware was necessary for RX-28. For the uncoupling in the lower torque range, e.g., the motor can execute an active back-set movement, or the coupling construction becomes optimized in that way, that the internal spring tension also with slightest torque is sufficient to generate a back-set movement.

By the use of the present coupling in rotary joints of robots, the possibility exists to decouple an actuator of the joint. This can especially increase the energy efficiency with pendulum's movements of a joint, because the actuator does not have to be moved continuously with it. Therefore, this application is especially useful for the joint actuation in walking robots because leg motions can be seen as similar to periodic swing

motions. Specifically in humanoid walking, the arms also perform a periodic swing motion for which the clutch can be useful. Up to the current measurement at the actuator, no further sensor, as well as no active switch signal for the coupling, is additionally necessary for the uncoupling. In order to stabilize the instable position of a joint, free from float, the use of two, parallel switched actuators is necessary. On this occasion, both motors would operate mutually to maintain the internal tension of both couplings. In addition, by the use of the coupling, actuators with different gear ration can be connected, without that the maximum speed of the joint is regulated by slowest actuator. Because the coupling guaranties the "overrun" of the drive shaft, an overstress of the actuator, in rotation direction of the actuator, is not possible. In addition, the actuator can be decoupled, e.g., while recognizing a fall. By reason of these both possibilities, the present coupling presents likewise a protection against the overstress.

REFERENCES

[1] M. Hild, T. Siedel, C. Benckendorff, M. Kubisch, and C. Thiele. Myon: concepts and design of a modular humanoid robot which can be reassembled during runtime. In *Proceedings of the 14th International Conference on Climbing and Walking Robots (CLAWAR)*, 2011.

[2] M. Hild, T. Siedel, and T. Geppert. Design of a passive, bidirectional overrunning clutch for rotary joints of autonomous robots. In *Proceedings of the 4th International Conference on Intelligent Robotics and Applications (ICIRA), (submitted)*, 2011.

[3] M. Holgerson. Apparatus for measurement of engagement characteristics of a wet clutch. *Wear*, 213(1-2):140–147, 1997.

[4] S. Klug, B. Möhl, O. Von Stryk, and O. Barth. Design and application of a 3 dof bionic robot arm. *regulation*, 11:12.

[5] K. Liu and E. Bamba. Frictional dynamics of the overrunning clutch for pulse-continuously variable speed transmissions: rolling friction. *Wear*, 217(2):208–214, 1998.

[6] K. Liu and E. Bamba. Analytical model of sliding friction in an overrunning clutch. *Tribology international*, 38(2):187–194, 2005.

[7] D. C. Ochab and J. R. Updyke. Bi-directional overrunning clutch, October 26 1999. US Patent 5,971,123.

[8] W.C. Orthwein. *Clutches and brakes: design and selection*. CRC, 2004.

[9] J.E. Pratt and B.T. Krupp. Series elastic actuators for legged robots. In *Proceedings of SPIE–The International Society for Optical Engineering*, volume 5422, pages 135–144, 2004.

[10] G.M. Roach and L.L. Howell. Evaluation and comparison of alternative compliant overrunning clutch designs. *Journal of Mechanical Design*, 124:485, 2002.

[11] M. Saiko. Bi-directional clutch, April 24 2002. EP Patent 1,199,490.